Molecular simulation of hierarchical structures in bent-core nematics

S. D. Peroukidis, A. G. Vanakaras and D. J. Photinos

Department of Materials Science, University of Patras, Patras 26504, GREECE

Supplementary Information

This supplementary information file consists of four sections: In section 1 we introduce the interaction potential used in the molecular simulations. In section 2 we define the ordering matrix tensors used in this study and describe the nematic phases in terms of them. In section 3 we present a set of calculated positional and mixed positional-orientational two-dimensional pair correlation functions. In section 4 we briefly describe the methodology for the calculation of the correlation lengths and we compare our results with available experimental results.

1. Interaction potential

A variant of the anisotropic soft-core potential introduced in Ref. [R1] is used to describe the interaction potential between the spherocylindrical segments. The repulsive part grows exponentially with distance, as opposed to the linear increase of the original form [R1], in order to prevent extensive overlapping of the segments. The functional form of the potential reads

$$U(d)=\begin{cases} \varepsilon+\exp\left(U_{max}\left(1-d\right)^2\right)-1 \;, & d<1 \\ U_{max}\left(1-d\right)^2-U_{attr}\left(\hat{u}_i,\hat{u}_j\right)\left(1-d\right)^4+\varepsilon, & 1\le d<d_{cut} \end{cases},$$

with $U(d)=0$ when $d>d_{cut}$; here, d, ε and d_{cut} are functions of the directions of the cylindrical segments and of the vector connecting their centers and denote respectively: the shortest distance (in units of D) between a pair of segments, the maximum well depth and the cut-off distance of the potential. The latter two are determined simultaneously by requiring the potential and its first derivative to vanish at the cut-off separation. Lastly, $U_{attr}\left(\hat{u}_i,\hat{u}_j\right)=U_0-5\varepsilon_2 P_2\left(\hat{u}_i\cdot\hat{u}_j\right)$, with P_2 denoting the 2nd Legendre polynomial. Introducing ε_0 as an energy unit that sets the scale for the reduced temperature according to $T^*=kT/\varepsilon_0$, we have chosen $U_0=150\varepsilon_0$,

$\varepsilon_2 = 12\varepsilon_0$ and $U_{\max} = 25\varepsilon_0$ which allow for a relatively broad stability range of the nematic phase. With this parameterization the potential-well depth for two parallel spherocylinders with their centers at a distance D apart, is $\sim -1.7\varepsilon_0$. Flexibility is readily introduced when $\theta \neq 0^o$, in which case each end-segment is allowed fixed-θ precessions about the long axis of the spherocylindrical core segment it is attached to (see Fig. 1(a) in the main text of the letter).

2. Ordering Matrix Tensors for the Nematic Phase

For a given configuration of the molecules within the simulation box, the principal axes $\hat{X}_p, \hat{Y}_p, \hat{Z}_p$ are determined through the diagonalization of the ordering matrix tensors [R2]

$$Q_{AB}^{\alpha\alpha} = \frac{1}{2N}\sum_{i=1}^{N}\left[3\left(\alpha_i.A\right)\left(\alpha_i.B\right) - \delta_{AB}\right] \qquad (1)$$

with $\alpha_i = \hat{x}_i$ or $\hat{y}_i$ or $\hat{z}_i$ representing the molecular axes of the *i*th molecule and $A, B = \hat{X}, \hat{Y}, \hat{Z}$ representing the axes of the simulation box. The three eigenvalues of the Q_{AB}^{zz} tensor are sorted according to sequence $\lambda_1^z > \lambda_2^z > \lambda_3^z$. In the untwisted nematic state, N^0, these satisfy the conditions $\lambda_1^z > 0$ and $\lambda_2^z \approx \lambda_3^z < 0$, in which case the nematic director ($\hat{n} \equiv \hat{Z}_p$) is identified as the eigenvector associated with λ_1^z. In the twisted states, $N^{\pm}$, the three eigenvalues satisfy $\lambda_1^z \approx \lambda_2^z > 0$, $\lambda_3^z < 0$ and the helix axis $\hat{h} \equiv \hat{Z}_p$ is taken to coincide with the eigenvector of λ_3^z. According to these assignments, the nematic order parameter is obtained as $S = \left\langle 3\left(\hat{z}_i \cdot \hat{Z}_p\right)^2 - 1 \right\rangle / 2$ and the biaxial order parameter as $B = \left\langle \left(\hat{x}_i \hat{X}_p\right)^2 - \left(\hat{x}_i \hat{Y}_p\right)^2 - \left(\hat{y}_i \hat{X}_p\right)^2 + \left(\hat{y}_i \hat{Y}_p\right)^2 \right\rangle / 2$.

In the N^0 phase, the order parameter $S = < 3\left(\hat{z}_i \cdot \hat{n}\right)^2 - 1 > /2$, is found to be around 0.7-0.8 at the $I-N$ transition and to increase with decreasing temperature. The biaxial order parameter in this phase is essentially zero throughout the nematic temperature range. To quantify the orientational order in the $N^{\pm}$ states we have divided the sample into thin slabs (thickness of 2-3 molecular diameters) normal to

the helix axis $\hat{h}$. The order parameter in each slab shows the same numerical values and temperature dependence with the global order parameter S found for the N^0 state. However, the biaxial order parameter within each slab takes clearly and persistently non-zero values, reflecting local biaxial order, as expected for a chiral state wherein the helix axis breaks the rotational symmetry about the nematic director.

3. Two-Dimensional Pair Correlation Functions

The usual radial pair correlation functions are not always sensitive for the detection the local structure around a molecule, either because they inherently entail averaging over spherical shells or because their calculation involves macroscopic properties (such as the nematic director) which could in fact fluctuate considerably. For instance, from the calculation of the usual radial pair correlation function $g(r)$ and the respective projected distributions $g_{\perp}(r_{\perp})$, $g_{//}(r_{//})$, it follows that the N^0 and the $N^{\pm}$ states exhibit purely positional correlations only over a relatively short range. These pair correlations, however, are not appropriate for detecting mixed positional and orientational correlations and therefore could not reveal clearly the presence of helical order. Thus, to analyze the nematic states at the microscopic level, i.e the local environment sensed by a single molecule, we have calculated the set of mixed positional/orientational two-dimensional pair correlation densities defined in the main text of the letter, which refer to molecular axis frames (as opposed to the director frames).

In Figs. S1 and S2 we present the calculated $g_{1;\hat{x}}^{\hat{a},\hat{b}}$ and $g_{0}^{\hat{a},\hat{b}}$ at relatively low temperature ($T^* = 2.2$) for the N^0 state for the three molecular planes (i.e the planes defined by the $x-y$, $x-z$ and $y-z$ molecular axes). In Figs. S3 and S4 we present the respective functions for the N^- state at the same temperature.

From the graphs of the $g_{0}^{\hat{x},\hat{y}}(x,y)$ functions, both in N^0 and N^- states (see Figs. S2(a) and S4(a)), it follows that the molecules surrounding a given molecule are arranged uniformly in the $x-y$ plane of that molecule. On the other hand, the $g_{1;\hat{x}}^{\hat{x},\hat{y}}(x,y)$ functions are strongly anisotropic (see Figs. S1(a) and S3(a)). Each molecule in the sample can be viewed as being surrounded by a non spherical region

containing neighboring molecules that have strong polar (and therefore biaxial) correlations with that molecule. The $g_0^{\hat{x},\hat{z}}(x,z)$ functions (see Figs. S2(b) and S4(b)) show secondary maxima (indicated by the red arrows) at separations equal to one molecular length, which indicates directly the tendency for layering. The sign-alternation of the $g_{1;\hat{x}}^{\hat{x},\hat{z}}(x,z)$ functions (see Figs. S1(b) and S3(b)) is evidence of antiferroelectric order.

4. Estimates of Correlation Lengths and Comparison with Experiment

The polar correlation lengths ξ_x, ξ_y along the $\hat{x}$ and $\hat{y}$ molecular axes, respectively, were estimated from $g_{1;\hat{x}}^{\hat{x},\hat{y}}(x,y)$ as the optimal parameters for fitting the separate x and y dependences of this function to the functional forms $g_{1;\hat{x}}^{\hat{x},\hat{y}}(x,0) \sim e^{-|x|/\xi_x}$ and $g_{1;\hat{x}}^{\hat{x},\hat{y}}(0,y) \sim e^{-|y|/\xi_y}$ (see Figs. S1(a) and S3(a)). The estimated uncertainties of the values of the correlation lengths ξ_x and ξ_y obtained with this procedure are $O\left(5\cdot 10^{-2}\right)$ at high temperatures and $O\left(5\cdot 10^{-1}\right)$ at lower temperatures. Roughly, the average transversal correlation length is estimated from $\xi_\perp \approx \left(\xi_x + \xi_y\right)/2$. The polar correlation length along the $\hat{z}$ molecular axis, ξ_z, has been estimated from fits to the functional dependence $g_{1;\hat{x}}^{\hat{x},\hat{z}}(x_{\max},z) \sim \cos\left(B_z z\right) e^{-|z|/\xi_z}$, which accounts for the simultaneous decay and sign change of $g_{1;\hat{x}}^{\hat{x},\hat{z}}(x_{\max},z)$ with z (see Figs. S1(b) and S3(b)). Here $x_{\max}$ denotes the position of the first maximum of $g_{1;\hat{x}}^{\hat{x},\hat{z}}(x,z)$; this is obtained at $x_{\max} = D$. The estimated uncertainty of the values obtained in this way for the correlation lengths ξ_z is $O\left(1\cdot 10^{-1}\right)$ at high temperatures and $O\left(2\cdot 10^{0}\right)$ at lower temperatures. The calculated polar correlation lengths, as functions of temperature, are shown in Fig. S5(a) for the N^0 and in Fig. S5(b) for the N^- state.

We have compared the values for the ratio $\xi_z/\xi_\perp$, as obtained from the calculations described above, with the values obtained from recent experimental XRD studies [R3, R4] on bent core molecules of the type we have modeled in our simulations. In Fig. S6 we present the calculated and the experimental values of the ratio $\xi_z/\xi_\perp$ as a

function of the reduced temperature $1-T/T_{IN}$, where T_{IN} is the isotropic-nematic transition temperature. Considering the simplicity of the molecular modeling, the agreement is remarkably good.

References of the supplementary file

[R1] J. S. Lintuvuori and M. R. Wilson, J. Chem. Phys. **128**, 044906 (2008).

[R2] P. J. Camp, M. P.Allen and A. J. Masters, J. Chem. Phys. **111**, 9871 (1999).

[R3] O. Francescangeli *et al.*, Adv. Funct. Mater. **19**, 2592 (2009).

[R4] O. Francescangeli and E. Samulski, Soft Matter **6**, 2413 (2010).

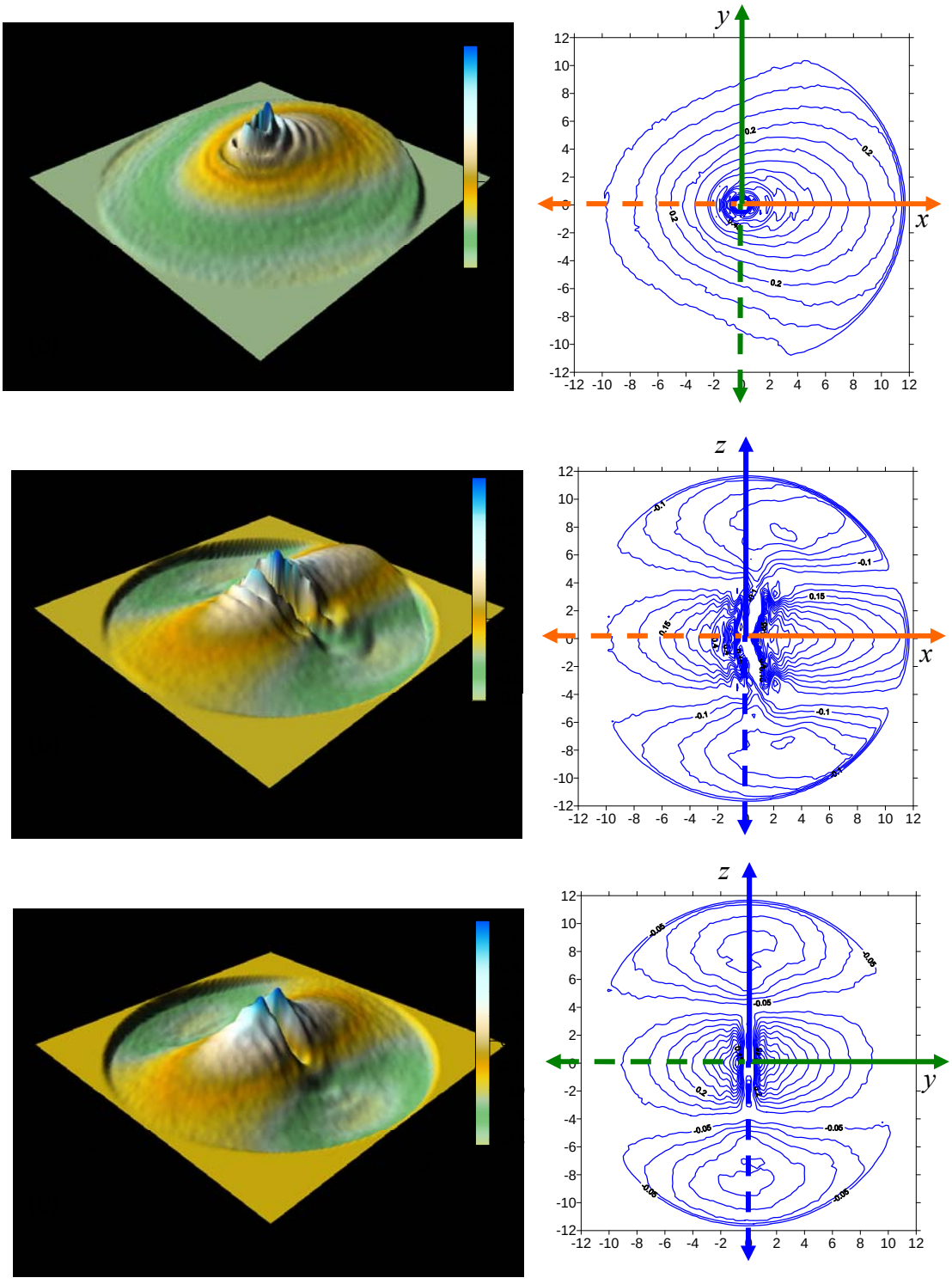

FIG. S1. Plots of the calculated correlation functions for the untwisted nematic state N^0 at temperature $T^* = 2.2$. (a) $g^{\hat{x},\hat{y}}_{1;\hat{x}}(x,y)$, (b) $g^{\hat{x},\hat{z}}_{1;\hat{x}}(x,z)$ and (c) $g^{\hat{y},\hat{z}}_{1;\hat{x}}(y,z)$. Left column: 3 dimensional plots; Right Column: contour plots.

(a)

(b)

(c)

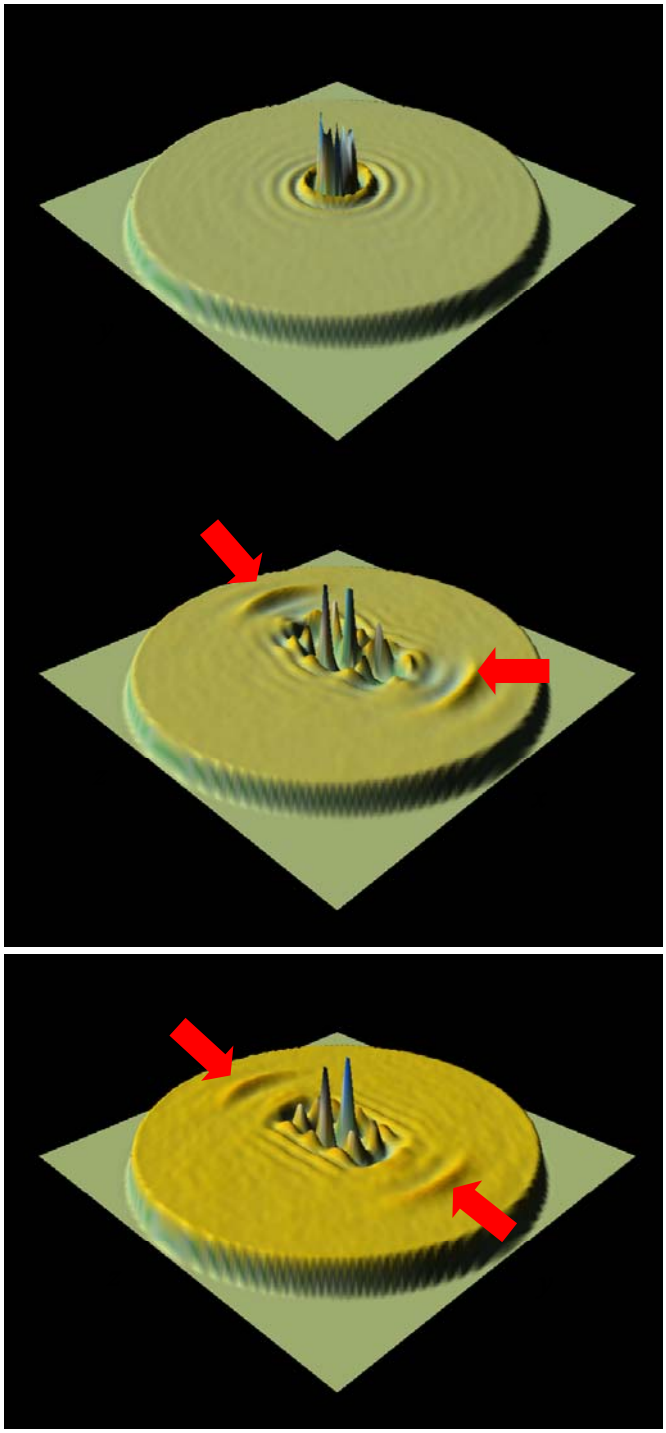

FIG. S2. Plots of the calculated correlation functions for the untwisted nematic state N^0 at temperature $T^* = 2.2$. (a) $g_0^{\hat{x},\hat{y}}(x,y)$, (b) $g_0^{\hat{x},\hat{z}}(x,z)$ and (c) $g_0^{\hat{y},\hat{z}}(y,z)$. The characteristic secondary maxima (indicated by arrows) suggest a tendency for layering.

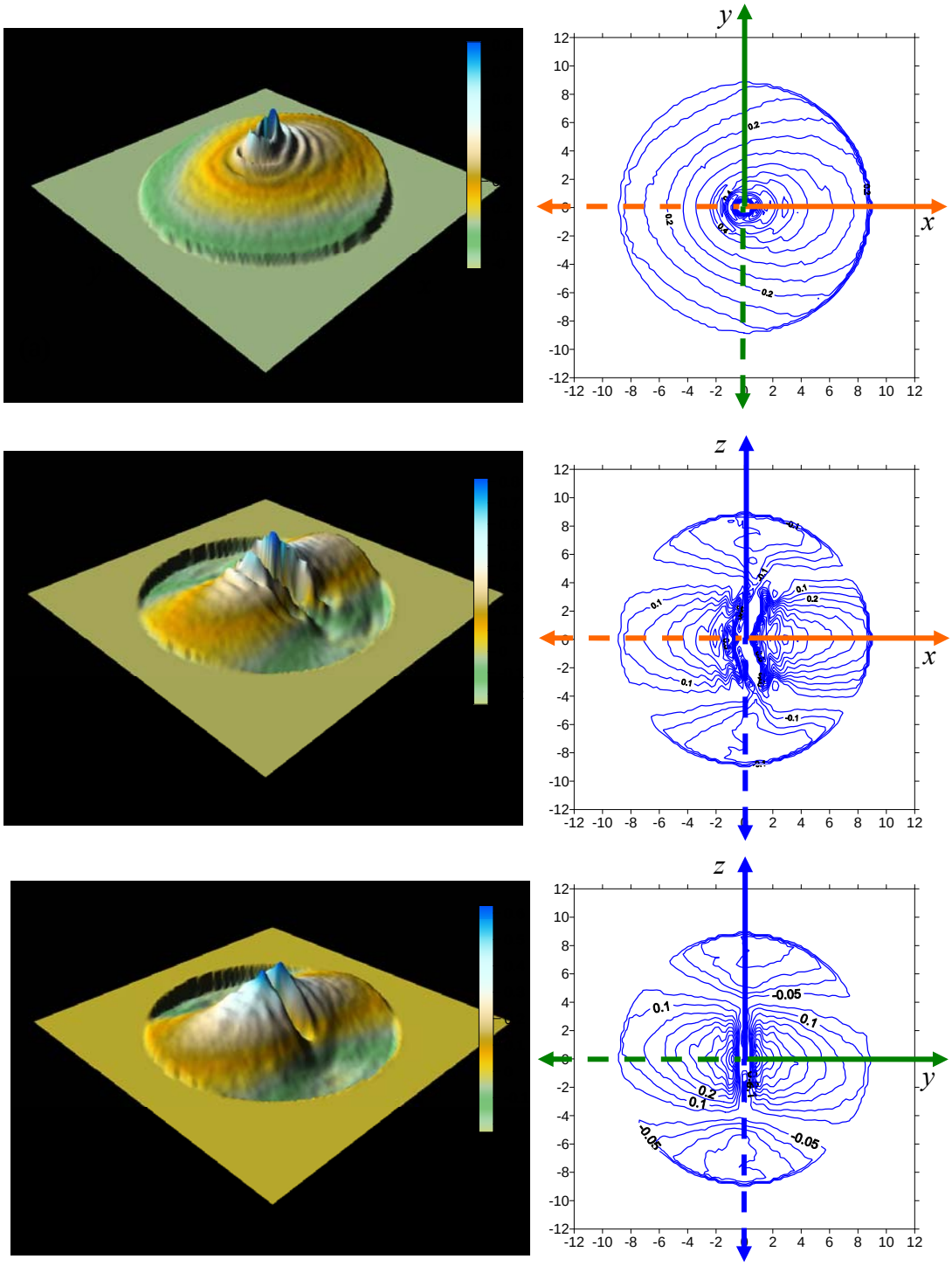

FIG. S3. Plots of the calculated correlation functions for the twisted nematic state N^{-} at temperature $T^{*}=2.2$. (a) $g_{1;\hat{x}}^{\hat{x},\hat{y}}(x,y)$, (b) $g_{1;\hat{x}}^{\hat{x},\hat{z}}(x,z)$ and (c) $g_{1;\hat{x}}^{\hat{y},\hat{z}}(y,z)$. Left column: 3 dimensional plots; Right Column: contour plots.

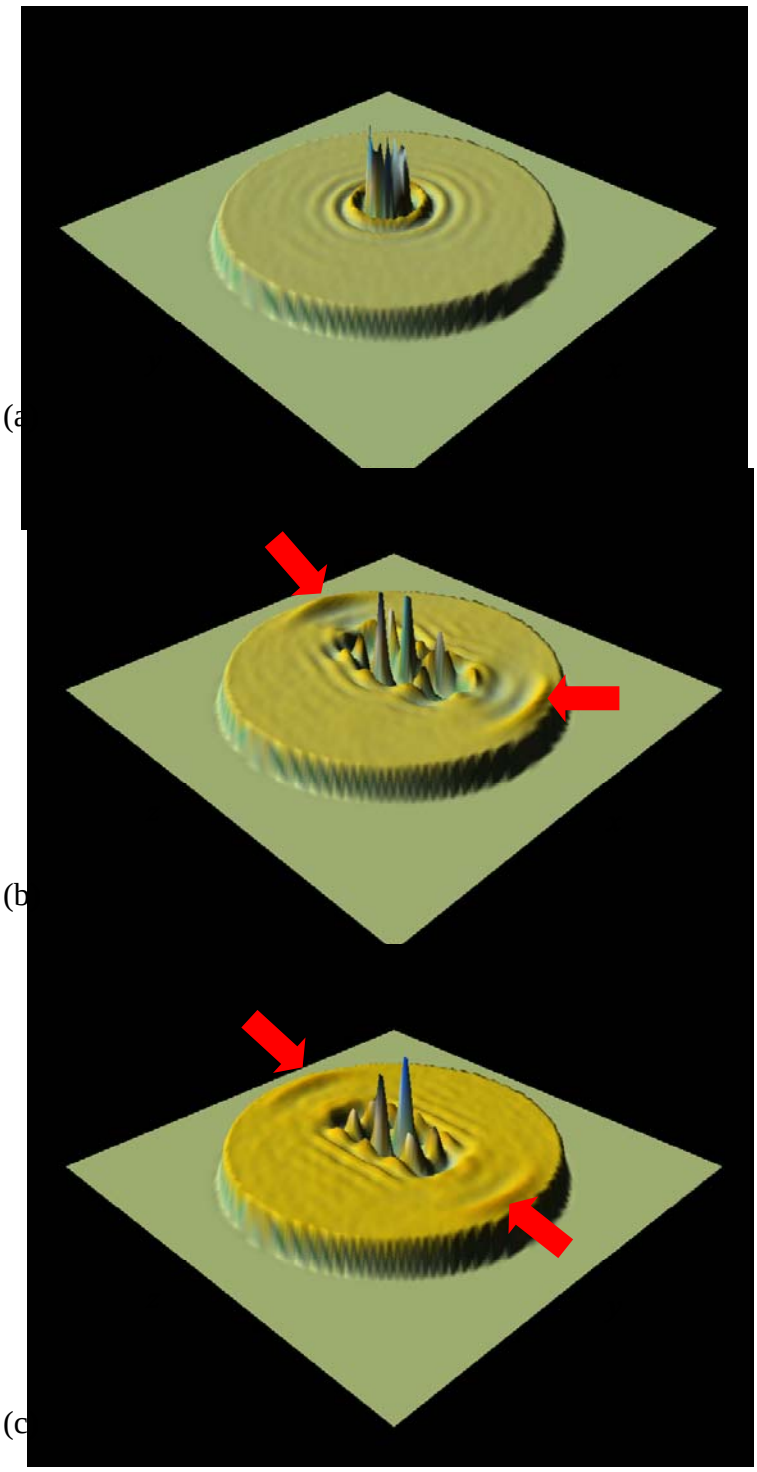

FIG. S4. Plots of the calculated correlation functions for the twisted nematic state N^{-} at temperature $T^{*}=2.2$. (a) $g_0^{\hat{x},\hat{y}}(x,y)$, (b) $g_0^{\hat{x},\hat{z}}(x,z)$ and (c) $g_0^{\hat{y},\hat{z}}(y,z)$. The characteristic secondary maxima (indicated by arrows) suggest a tendency for layering.

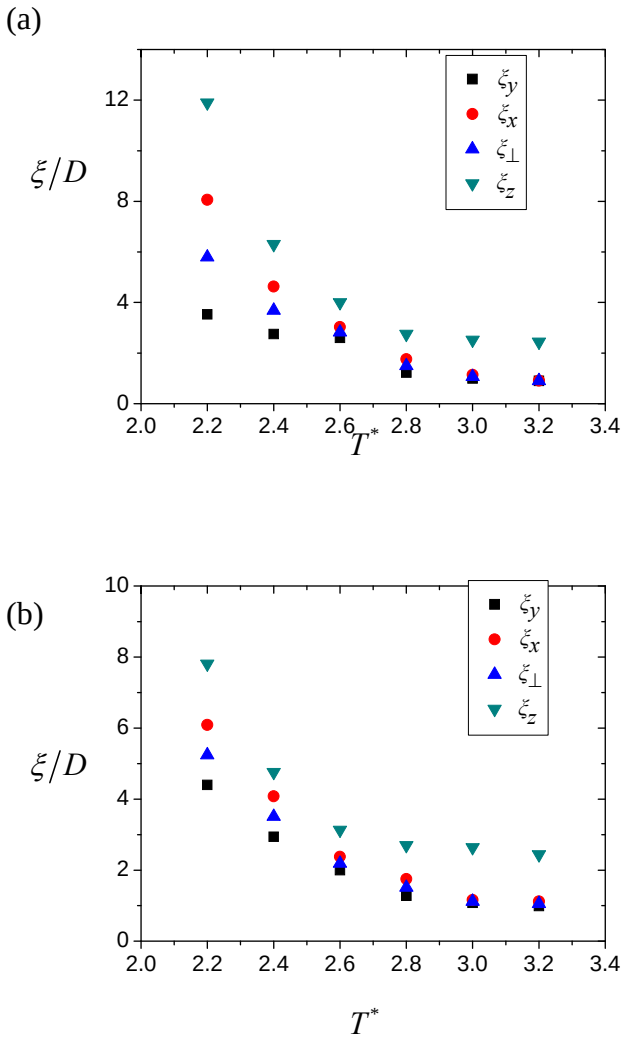

FIG. S5. Calculated temperature dependence of the polar correlation lengths ξ_x, ξ_y, ξ_z and $\xi_\perp$ for the untwisted nematic N^0 (a) and for the twisted nematic N^- (b).

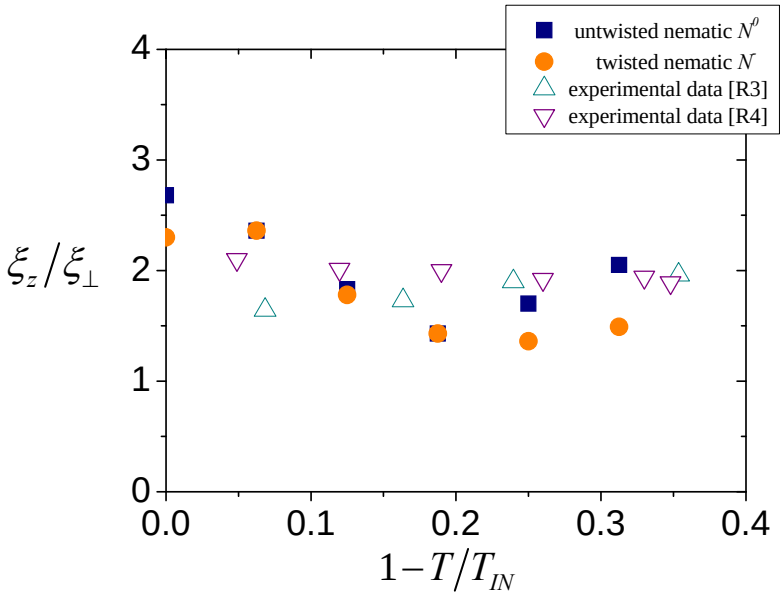

FIG. S6. Correlation length ratio $\xi_z/\xi_\perp$ as a function of the reduced temperature $1-T/T_{IN}$, where T_{IN} is the isotropic-nematic transition temperature. Calculated values from *MC*-NpT simulations are shown as squares (for the untwisted nematic N^0 state) and as circles (for the twisted nematic state N^-). Values obtained from XRD experiments are shown as upright triangles (data of Francescangeli et. al. [R3]) and as inverted triangles (data from Francescangeli and Samulski [R4]).